

DynFOA: Generating First-Order Ambisonics with Conditional Diffusion for Dynamic and Acoustically Complex 360-Degree Videos

Ziyu Luo¹Lin Chen¹Qiang Qu²Xiaoming Chen¹Yiran Shen³¹School of Computer and Artificial Intelligence, Beijing Technology and Business University, Beijing, China²School of Computer Science, The University of Sydney, Sydney, NSW, Australia³School of Software, Shandong University, Jinan, China

vincent.qu@sydney.edu.au, xiaoming.chen@btbu.edu.cn, yiran.shen@sdu.edu.cn

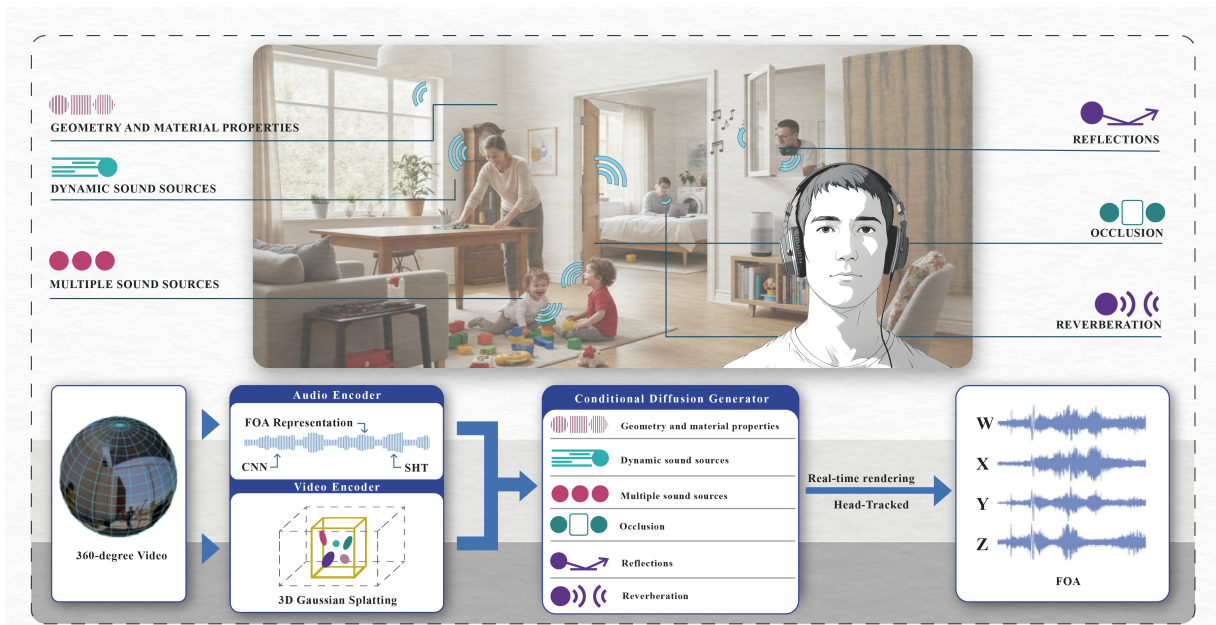


Figure 1: DynFOA Framework for Immersive First-Order Ambisonics (FOA) Generation. This pipeline processes 360-degree video input through a multi-stage architecture: video preprocessing and segmentation, multi-modal feature extraction using Convolutional Neural Networks (CNN) for visual features and Spherical Harmonic Transform (SHT) for spatial audio decomposition, cross-modal feature fusion and alignment, geometric and acoustic scene analysis for material property estimation, and spatially-aware sound source separation. The conditional diffusion generator then integrates these extracted features—including geometry, material properties, and localized sound sources—with physics-based acoustic modeling to generate high-fidelity FOA audio featuring realistic occlusion, reflections, and reverberation effects, delivering an immersive spatial audio experience.

ABSTRACT

Spatial audio is crucial for creating compelling immersive 360-degree video experiences. However, generating realistic spatial audio, such as first-order ambisonics (FOA), from 360-degree videos in complex acoustic scenes remains challenging. Existing methods often overlook the dynamic nature and acoustic complexity of 360-degree scenes, fail to fully account for dynamic sound sources, and neglect complex environmental effects such as occlusion, reflections, and reverberation, which are influenced by scene geometries and materials. We propose DynFOA, a framework based on dynamic acoustic perception and conditional diffusion, for generating high-fidelity FOA from 360-degree videos. DynFOA first performs visual processing via a video encoder, which detects and localizes multiple dynamic sound sources, estimates their depth and semantics, and reconstructs the scene geometry and materials using a 3D Gaussian Splatting. This reconstruction technique accurately models occlusion, reflections, and reverberation based on the geometries and materials of the reconstructed 3D scene and the listener’s viewpoint. The audio encoder then captures the spatial motion and temporal 4D sound source trajectories to fine-tune the diffusion-

based FOA generator. The fine-tuned FOA generator adjusts spatial cues in real time, ensuring consistent directional fidelity during listener head rotation and complex environmental changes. Extensive evaluations demonstrate that DynFOA consistently outperforms existing methods across metrics such as spatial accuracy, acoustic fidelity, and distribution matching, while also improving the user experience. Therefore, DynFOA provides a robust and scalable approach to rendering realistic dynamic spatial audio for VR and immersive media applications.

Index Terms: 360-Degree Video, First-Order Ambisonics, DynFOA, Conditional Diffusion.

1 INTRODUCTION

Spatial audio is a cornerstone of immersion in Virtual Reality (VR) and 360-degree media, allowing users to perceive sound with realistic direction, distance, and environmental context [41]. Unlike conventional stereo audio, spatial audio aligns the auditory environment with visual cues, enabling a coherent perceptual scene. However, generating high-fidelity, physically plausible spatial audio remains challenging. Realistic spatial audio requires not only precise

synchronization with visual events but also accurate 3D localization of sound sources, realistic modeling of occlusion, reflections, and reverberation, and adaptation to the listener’s head orientation in real time [13].

A major limitation in existing works is the under-utilization of the rich geometric and semantic information available in 360-degree video for audio rendering. Many methods, such as some FOA-based approaches or hybrid audio-visual models, focus primarily on sound source localization without modeling how the surrounding environment shapes the sound field. For instance, OmniAudio [32] generates FOA audio but assumes static, context-free sound sources, while Sonic4D [36] estimates 3D positions but outputs only stereo audio, reducing immersion. These approaches typically neglect how environmental factors, such as moving objects, walls, or furniture, affect propagation through occlusion, reflections, and reverberation. This omission results in sound fields that lack physical grounding and fail to adapt convincingly to user orientation.

To address these limitations, we present **DynFOA**, a geometry- and material-aware FOA generation framework for 360-degree videos. Our method explicitly reconstructs the scene’s 3D geometry from monocular 360-degree video using a pipeline consisting of sound source detection, dense depth estimation, semantic segmentation, and 3D Gaussian Splatting (3DGS) reconstruction. The resulting geometry is augmented with per-surface material properties to derive acoustic descriptors, including occlusion masks, reflection paths, and frequency-dependent reverberation times. These descriptors serve as conditioning signals for a diffusion-based FOA generator, enabling audio rendering that responds dynamically to both the spatial structure of the scene and the listener’s head orientation. By conditioning the denoising process on real scene geometry, DynFOA produces physically consistent spatial audio that preserves directionality, distance cues, and environmental characters. Our evaluations demonstrate that DynFOA not only achieves superior spatial accuracy, acoustic fidelity, and distribution matching compared to existing methods, but also provides a more engaging user experience.

Our key contributions are summarized as follows:

- **Visual-Acoustic Scene Reconstruction:** We introduce a visual processing pipeline that reconstructs scene geometry and materials from 360-degree video, enabling physically grounded modeling of occlusion, reflections, and reverberation effects in spatial audio rendering.
- **Conditional Diffusion for FOA Generation:** We design a conditional diffusion model operating in the latent FOA domain, where denoising steps are guided by geometry- and material-aware acoustic descriptors, allowing spatial audio to adapt naturally to listener orientation and viewpoint changes.
- **Special Datasets:** We create a comprehensive dataset Dyn360 for complex acoustic scenes with occlusion, reflections, and reverberation, which contains 600 video scenes and three sub-datasets of their content in Sec. 4.1.1.
- **Comprehensive Evaluation:** We establish an extensive evaluation framework specifically targeting Dyn360 as a comprehensive benchmark, and experiments demonstrated that our DynFOA achieved state-of-the-art performance in both quantitative and qualitative analysis.

By uniting physically grounded scene reconstruction with diffusion-based generative modeling, DynFOA advances spatial audio rendering beyond purely perceptual alignment toward true audiovisual physical coherence, offering a new pathway for immersive media production in VR and cinematic 360-degree experiences.

2 RELATED WORK

2.1 Spatial Audio Representations and Rendering

Spatial audio reproduction in VR has long relied on Ambisonics, which encodes sound fields in the spherical harmonic domain [19]. First-Order Ambisonics (FOA) strikes a balance between spatial resolution and computational efficiency, while higher-order Ambisonics improves angular precision at a higher computational cost. The mathematical foundation of spherical harmonic decomposition allows for 3D sound field capture and reconstruction at varying levels of accuracy, making Ambisonics particularly well-suited for VR, where perceptual fidelity must be balanced with real-time processing constraints.

For spatial audio rendering, Head-Related Transfer Functions (HRTFs) are essential, providing the necessary filtering to simulate spatial localization. Standardized resources, such as KEMAR [17] and CIPIC [1], along with exchange formats like SOFA [22], form the foundation for HRTF-based rendering. However, individualization remains a challenge due to anthropometric variability, which affects localization and externalization of sounds. Recent works have addressed this issue through both direct measurements and computational models. Platforms for acoustic simulation, such as SoundSpaces [5, 6], offer 3D scanned environments with physically-grounded propagation models, enabling systematic evaluation and cross-modal learning. These platforms emphasize the importance of jointly modeling visual and acoustic cues for better audio-visual scene understanding. In the context of 360-degree video, early work [35] generated FOA from mono audio, using panoramic cues. OmniAudio [32] formalized the 360V2SA task, but with the assumption of static sources and negligible occlusion or reverberation. Sonic4D [36] reconstructed dynamic 3D trajectories for viewpoint-adaptive binaural rendering, though it did not produce FOA. More recent geometry-aware methods [37, 33] leverage depth cues, but they typically focus only on source distance.

However, these existing works have not sufficiently considered the influence of scene geometry and materials, which affect occlusion, reflections, and reverberation, in the generation of FOA for complex scenes involving dynamic sound sources.

2.2 Cross-Modal Learning for Sound Localization and Separation

Cross-modal learning leverages the synergy between different modalities: visual signals help constrain sound localization and disambiguate overlapping events, while audio assists in grounding visual understanding. This synergy is particularly crucial for immersive spatial audio, where multiple sound sources and complex environments necessitate robust sound separation. A significant body of work has explored cross-modal learning for sound localization and separation using visual cues. Weakly supervised methods align objects with sounds [2, 40, 38], while co-separation frameworks learn to disentangle multiple overlapping sound sources. Other approaches focus specifically on speech, such as speaker-independent audiovisual separation [14] and lip-synchronized speech extraction [16]. Large-scale datasets like AudioSet [18], VGGSound [11], and MUSIC [56] have significantly accelerated these advances by providing diverse audio-visual training resources.

Our framework builds on these principles but extends them to FOA generation. By integrating monocular 360-degree vision with geometry- and material-aware acoustic descriptors, we enable sound localization and separation in acoustically complex environments, where traditional cross-modal methods often fall short.

2.3 Visually Guided Spatialization for 360-Degree Video

Recent advancements have focused on vision-guided audio spatialization. Early approaches addressed mono-to-binaural conversion using neural networks [15], while later works shifted toward stereo or pseudo-binaural generation [48]. Methods like Points2Sound

incorporated geometry and motion cues to improve spatialization [33], and newer pipelines introduced explicit depth estimation or scene reconstruction for greater accuracy. Despite these developments, many approaches still oversimplify acoustic propagation, often assuming free-field conditions or modeling only distance attenuation. To address this, OmniAudio [32] and Sonic4D [36] made significant progress by targeting panoramic or dynamic sources. However, they did not account for FOA outputs or more complex propagation effects, such as reverberation. Head-tracked playback pipelines further demonstrated the necessity of synchronizing audio rotation with the listener’s orientation, but they remain limited in handling occlusion and material diversity.

To overcome these limitations, we leverage 360-degree scene reconstruction with per-surface material estimation. By modeling occlusion, reflections, and reverberation, we condition FOA generation on physically meaningful descriptors, enabling both head-tracked adaptability as well as geometry- and material-aware spatial realism.

2.4 Diffusion Models for High-Fidelity Audio Generation

Generative models have recently revolutionized audio synthesis. Diffusion models, such as WaveGrad [7], DiffWave [25], and AudioGen [26], have set new benchmarks in waveform generation. Spatial audio frameworks based on diffusion, such as DiffSAGe [27] and ImmerseDiffusion [20], demonstrate strong potential, though they focus primarily on perceptual fidelity rather than ensuring physical scene consistency. Meanwhile, autoregressive models like SoundStorm [3] and controllable music generators [12] offer sequence-level control but struggle with long-term coherence. Video-to-audio pipelines, such as ViSAGe [24] and MMAudio [10], integrate motion and semantic cues but rarely address FOA generation or physically grounded propagation.

DynFOA addresses these gaps by embedding geometry- and material-aware descriptors into a conditional diffusion pipeline for FOA generation. This approach enables us to combine the high-fidelity synthesis capabilities of diffusion models with explicit modeling of occlusion, reflections, and reverberation, advancing generative spatial audio from perceptual plausibility to physical consistency.

3 METHODOLOGY

3.1 Problem Definition

The objective of this work is to enable **physically grounded and perceptually coherent 4D immersive experiences** from 360-degree videos by learning to **generate scene-aware spatial audio**. Prior approaches to spatial audio rendering often rely on simplified acoustic assumptions, neglecting critical aspects such as dynamic sound sources, concurrent source interactions, and propagation effects including occlusion, reflections, and reverberation. Our framework, **DynFOA**, directly addresses these challenges by learning from multimodal cues—visual appearance, 3D geometry, and material properties—to synthesize first-order ambisonics (FOA) that faithfully reflect the physical structure and acoustic conditions of the scene [31, 26].

Formally, we cast this task as learning a mapping:

$$f_{\theta} : (V, G, M, R, \mathbf{o}) \mapsto S_{4D}, \quad (1)$$

where V is the 360-degree video stream, G denotes the reconstructed 3D scene geometry, M represents per-surface material properties, R encodes reverberation and reflection parameters, and \mathbf{o} specifies the listener’s head orientation. The learnable function f_{θ} , parameterized by θ , integrates these modalities to generate a multi-modal 4D representation S_{4D} , in which spatially aligned audio and visual cues jointly define the immersive experience.

Solving this problem requires addressing a sequence of coupled sub-tasks across both the visual and audio domains. On the visual side, the model must (i) detect and localize sound-emitting and non-emitting objects, (ii) estimate depth, (iii) perform semantic segmentation, and (iv) reconstruct a geometry- and material-aware 3D representation using techniques such as 3D Gaussian Splatting (3DGS) [50, 55]. On the audio side, the model must (i) extract directional cues from FOA channels, (ii) encode them into a latent representation, and (iii) model complex propagation phenomena including occlusion, reflections, and reverberation [31, 47].

The key challenge lies not only in localizing sound sources but also in handling multiple, dynamic sources within acoustically complex environments [23]. By grounding audio generation in geometry- and material-aware acoustic descriptors, our model captures both static and dynamic elements of the scene. This enables real-time adaptation to source motion, ensuring accurate localization, separation, and a physically consistent audio field that reflects the spatial relationships inherent in 360-degree visual scenes [8].

3.2 Overview

Figure 2 illustrates the proposed DynFOA framework, which generates dynamic and physically consistent first-order ambisonics (FOA) from 360-degree video. The model consists of three modules: a **Video Encoder**, an **Audio Encoder**, and a **Conditional Diffusion Generator**. The **Video Encoder** (Sec. 3.3) reconstructs 3D scene geometry and material properties from 360-degree video. It detects and tracks dynamic sound sources, estimates depth, and applies semantic segmentation, producing geometry- and material-aware acoustic descriptors such as occlusion, reflections, and reverberation. The **Audio Encoder** (Sec. 3.4) processes FOA signals into geometry-aware embeddings. Through spectral decomposition, spherical harmonic transformation, and spatial mapping, it captures directional cues, attenuation, and material absorption, while integrating saliency and reverberation features for consistency with the visual scene. At the core, the **Conditional Diffusion Generator** (Sec. 3.5) fuses video- and audio-derived features via a multi-condition encoder. Geometry, material, and propagation cues—along with descriptors of dynamic and multiple sound sources—guide a U-Net denoiser to synthesize FOA that are both physically grounded and perceptually realistic. During inference, the generated FOA is rotated according to the listener’s head orientation and rendered binaurally with HRTFs, enabling real-time, head-tracked playback with immersive spatial audio.

3.3 Video Encoder

The Video Encoder extracts spatial and semantic cues from 360-degree video to support realistic sound propagation modeling and synchronized spatial audio rendering [44, 51]. It operates in three stages: (1) sound source localization and depth estimation, (2) semantic segmentation and scene reconstruction, and (3) feature extraction and multi-modal fusion.

3.3.1 Sound Source Localization and Depth Estimation

The encoder first detects and localizes sound-emitting objects in the scene [29]. Each source i is assigned a bounding box \hat{b}_i and an activity score \hat{y}_i , optimized by:

$$\mathcal{L}_{obj} = \sum_i \left(\|b_i - \hat{b}_i\|^2 + (y_i - \hat{y}_i)^2 \right), \quad (2)$$

where b_i and \hat{b}_i denote the ground truth and predicted spatial parameters, while $y_i \in \{0, 1\}$ and $\hat{y}_i \in [0, 1]$ represent the true and predicted activity status. This ensures accurate detection and temporal tracking of dynamic sound sources.

Depth estimation then back-projects pixel-level depth into 3D points:

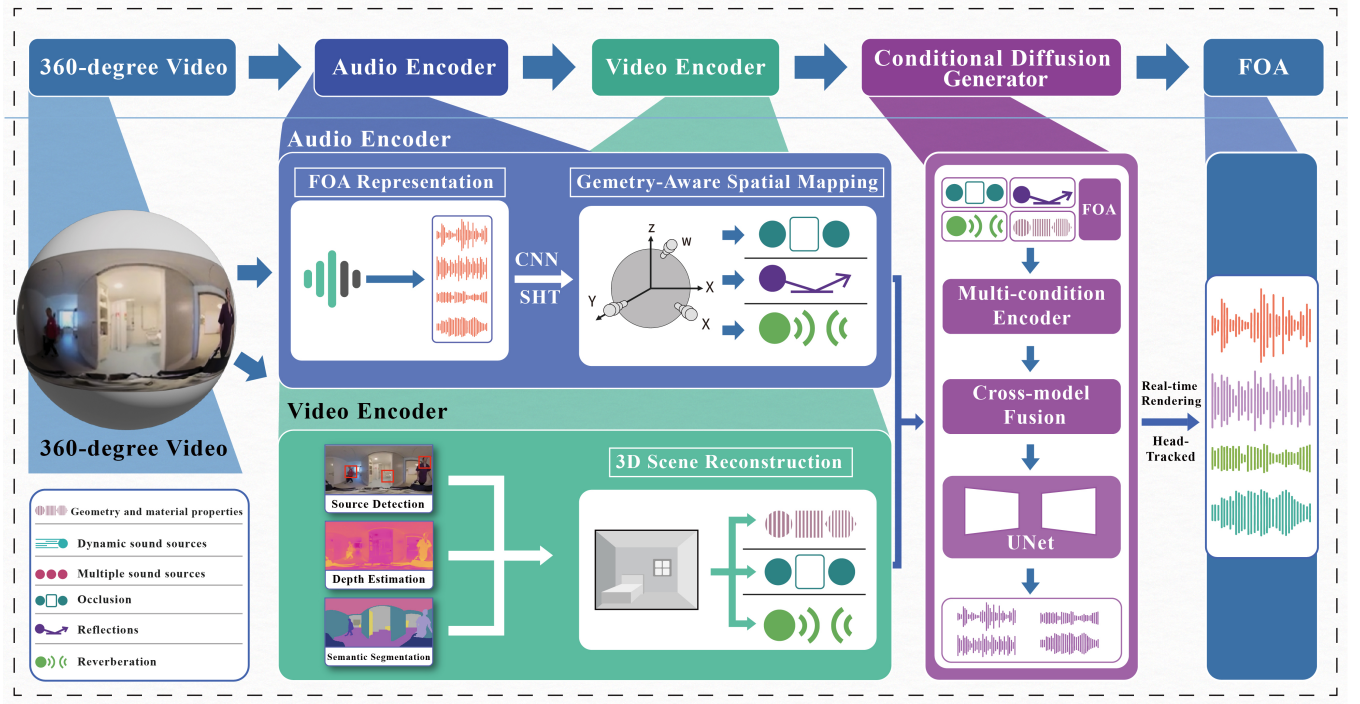


Figure 2: Overview of Our DynFOA. The model features a three-core architecture: audio encoder, video encoder, and conditional diffusion generator. The audio encoder enhances FOA audio robustness against occlusion, reflections, and reverberation through dynamic sound source processing. The video encoder reconstructs video information to support immersive FOA experiences. The conditional diffusion integrates scene context for deep FOA encoding and multimodal fusion, enabling real-time, high-fidelity immersive FOA rendering in scenes with occlusion, reflections, and reverberation.

$$p(u, v) = D(u, v) [\cos(\theta) \cos(\phi), \sin(\theta), \cos(\theta) \sin(\phi)]^T, \quad (3)$$

where (u, v) are image coordinates, $D(u, v)$ is depth, and θ, ϕ are the corresponding elevation and azimuth angles. The resulting point cloud serves as the geometric basis for acoustic modeling. To reconstruct the full scene, a hybrid approach combines Truncated Signed Distance Functions (TSDF) for large-scale structures with 3D Gaussian Splatting (3DGS) for fine details [49], enabling accurate modeling of occlusion, reflections, and reverberation.

3.3.2 Semantic Segmentation and Scene Reconstruction

The encoder further applies semantic segmentation to classify scene elements (e.g., walls, floors, furniture). Each class is mapped to frequency-dependent acoustic material properties [39, 46], enriching the reconstructed geometry with absorption and reflection parameters. These semantic and geometric cues are integrated into a 3D scene model [9], enabling simulation of occlusion, reflections, and reverberation based on both structure and material characteristics. This ensures that environmental effects such as sound blocking, scattering, and decay are faithfully captured.

3.3.3 Feature Extraction and Fusion

Finally, spatial and temporal features are extracted using Convolutional Neural Networks (CNNs) and Recurrent Neural Networks (RNNs) [42]. These video-derived features are fused with audio representations to jointly model scene dynamics and acoustic conditions. The resulting multimodal features support real-time tracking of dynamic sound sources while incorporating propagation effects (occlusion, reflections, and reverberation), thereby enabling perceptually coherent and immersive spatial audio rendering.

3.4 Audio Encoder

The Audio Encoder processes FOA signals to extract directional, spectral, and temporal cues that align with the geometry- and material-aware representations produced by the Video Encoder. By coupling FOA features with reconstructed scene properties, it enables context-aware spatialization consistent with the physical layout and acoustic characteristics of the environment [28, 52].

3.4.1 FOA Extraction and Normalization

We begin by extracting the four FOA channels, W , X , Y , and Z , which jointly represent omnidirectional and directional components of the sound field. To stabilize training and ensure consistent scaling across channels, z-score normalization is applied by subtracting the mean and dividing by the standard deviation of each channel. This reduces magnitude imbalance and provides a robust foundation for downstream feature learning.

From the normalized channels, a CNN extracts compact representations of spectral and directional patterns. Convolutions over the time-frequency domain capture harmonic content and inter-channel correlations, while stacked layers aggregate these into higher-level spatial features [42]. The resulting FOA embeddings form the basis for geometry-aware mapping and materially consistent spatial audio generation.

3.4.2 Spatial and Directional Mapping

To incorporate structural priors, we modulate FOA features with geometric distance and material-dependent absorption [28]. This accounts for sound attenuation and redirection during propagation:

$$A_{\text{path}} = \prod_j (1 - \alpha_{mj}) \cdot e^{-\gamma d}, \quad (4)$$

where α_{mj} is the absorption coefficient of the j -th material along the path, d is the propagation distance, and γ is the air attenuation

factor. This formulation supports the modeling of occlusion, early reflections, and late reverberation.

Directional information is further captured by projecting FOA features onto a spherical harmonic basis, yielding a compact representation of spatial energy distributions [45]. This transformation reinforces alignment between audio embeddings and reconstructed scene geometry, enabling accurate reasoning about sound propagation across directions.

3.4.3 Saliency, Reverberation, and Output

To highlight perceptually relevant cues, an attention mechanism modulates FOA features with visual saliency and acoustic context [52]:

$$a_t = \sigma(W_{\text{att}}[F_{\text{enc}}; M_{\text{vis}}] + b_{\text{att}}), \quad (5)$$

where $[F_{\text{enc}}; M_{\text{vis}}]$ concatenates encoded FOA features and visual saliency maps, W_{att} and b_{att} are learnable parameters, and σ is the sigmoid function. This selective amplification refines geometry- and material-aware features, enhancing the simulation of occlusion, reflections, and reverberation.

Spatial realism is further enriched by augmenting FOA features with late reverberation profiles that capture long-range energy decay and diffusion [46, 57]. Estimated from reconstructed geometry and material properties, these profiles complement direct sound and early reflections, yielding acoustically consistent reverberation patterns.

The Audio Encoder ultimately produces a geometry- and material-aware FOA embedding that is decoded into the four output channels. This representation preserves directional, spectral, and temporal consistency while remaining aligned with scene geometry, ensuring that the rendered spatial audio is both physically grounded and perceptually coherent.

3.5 Conditional Diffusion Generator

Inspired from recent spatial audio diffusion frameworks such as Diff-SAGe [27] and ImmerseDiffusion [20], we employ a conditional diffusion model to synthesize FOA that remain consistent with reconstructed scene geometry and material properties. Operating in the latent FOA domain, the model integrates structural and acoustic cues—including occlusion, reflections, and reverberation—while accounting for dynamic and multiple sound sources. Starting from a noisy latent representation, a U-Net denoiser progressively reconstructs clean FOA signals over T timesteps. Training follows the denoising diffusion probabilistic model (DDPM) objective:

$$\mathcal{L}_{\text{diff}} = \mathbb{E}_{x_0, \varepsilon \sim \mathcal{N}(0, 1), t} \left[\|\varepsilon - \varepsilon_{\theta}(x_t, t, c)\|_2^2 \right], \quad (6)$$

where x_t is the noisy FOA latent at timestep t , ε denotes Gaussian noise, ε_{θ} is the U-Net denoiser, and c is a conditioning vector that aggregates scene and propagation features.

3.5.1 Conditioning on Geometry and Material Properties

Reconstructed geometry and material attributes provide the foundation for physically grounded synthesis. The 3D mesh encodes structural layout and surface orientation, while material properties specify frequency-dependent absorption coefficients [46, 53]. Embedding these features allows the model to account for attenuation, diffraction, and spatial filtering effects, thereby ensuring that the generated FOA is consistent with the reconstructed scene. Such conditioning is particularly important in scenarios involving dynamic or multiple sound sources, where accurate modeling of energy interaction with the environment is essential.

3.5.2 Conditioning for Occlusion, Reflections, and Reverberation

To capture realistic propagation effects, the model is further conditioned on occlusion, reflections, and reverberation. Occlusion features are derived from visibility analysis between listener and sources, modulated by material absorption. Early reflections are estimated by tracing geometric paths, providing echo-like cues that enhance spatial depth. Reverberation is represented using frequency-dependent $T_{60}(f)$ curves, which describe late decay characteristics [20, 34]. Together, these cues enrich the conditioning stream, enabling FOA synthesis that incorporates both direct sound and its environmental response.

3.5.3 Multi-Condition Encoder and Cross-Modal Fusion

All conditional features are projected into a shared latent space before being injected into the diffusion U-Net. Modulation layers and cross-attention mechanisms fuse geometry, material, and propagation cues with descriptors of dynamic and multiple sound sources [43]. This cross-modal integration guides the denoising trajectory, ensuring that the generated FOA respects physical propagation constraints while maintaining perceptual consistency across time and sources.

3.5.4 Runtime Rendering and Head-Tracking

At inference, the diffusion model generates FOA conditioned on the reconstructed scene and dynamic context. The synthesized FOA signals are rotated according to the listener’s head orientation to maintain spatial alignment under head tracking [52, 28]. Finally, FOA are rendered to binaural signals using head-related transfer functions (HRTFs). This runtime process produces immersive spatial audio that adapts seamlessly to listener movement and complex multi-source environments.

4 EXPERIMENT

4.1 Experiment Setup

4.1.1 Dataset Usage and Construction

Our experiment is conducted based on the YT360 and Sphere360 datasets [32], and uses a bilingual Chinese and English keyword semantic filtering algorithm combined with a manual review mechanism to construct our **Dyn360** dataset. This dataset contains 600 strictly screened high-quality video clips that have been optimized to accurately reconstruct spatial audio in complex acoustic environments. All samples are normalized to 10 seconds in length, encoded in H.264 format, with a resolution of at least 720p and a stable frame rate of 30fps. The audio data is stored at a 16kHz sampling rate, 16-bit depth, and 4-channel format to generate high-quality FOA. All of the 600 clips are used for our quantitative evaluation reported later in Sec. 4.3.

To conduct more targeted research, we employed a combination of keyword identification and content-based filtering to categorize the source material into three distinct sub-datasets. First, as different geometric shapes exert distinct influences on the quality of FOA generation, we constructed a geometry sub-dataset (**Geometry**) by extracting video segments containing geometric elements, including basketballs and boxes in the same scene (corresponding to circles and squares with their respective different materials). This sub-dataset is designed to investigate how different geometries affect spatial audio rendering, and it contains 365 clips encoded in H.264 format at 640×360 resolution and 18.70 fps. Second, we established the move sound source sub-dataset (**MoveSource**) through manual curation of dynamic scenes featuring moving objects such as vehicles and pedestrians. This sub-dataset provides controlled conditions for analyzing occlusion and material-dependent propagation effects in dynamic environments, comprising 128 clips in H.264 format at 640×360 resolution and 29.01 fps. Third, we developed

the multi-sound source sub-dataset (**MultiSource**) by aggregating complex acoustic scenes containing two or more distinct sound sources. This sub-dataset emphasizes challenges such as reflections and reverberation in multi-source scenarios, yielding 107 clips in H.264 format at 640×360 resolution and 12.45 fps. All source videos underwent standardized preprocessing to comply with our Dyn360 specifications, including upsampling to a minimum resolution of 720p, frame rate normalization to 30fps, and segmentation into 10-second clips, thereby enabling comprehensive evaluation of our model’s adaptability across diverse scene complexities including occlusion, reflections, and reverberation.

4.1.2 Evaluation Metrics

We evaluated the FOA generation quality from our DynFOA and baselines along four different dimensions: spatial accuracy, acoustic fidelity, audio distribution matching, and user study protocol. Our evaluation metrics is specifically designed to validate the effectiveness of our DynFOA in handling complex acoustic scenarios, including occlusion, reflections, and reverberation.

Spatial accuracy evaluates the directional accuracy of the generated FOA using Direction of Arrival (DOA) estimation [58], which measures the angular accuracy of the predicted sound source positions relative to the true source positions in 3D space.

Acoustic fidelity assesses different model’s ability to capture complex acoustic environments, using Signal-to-Noise Ratio (SNR) [4] to measure audio clarity in the presence of background noise, and Early Decay Time (EDT) [30] to assess reverberation characteristics in various acoustic spaces, following established practices in spatial audio evaluation.

Audio distribution matching evaluates the similarity of feature distributions between real and generated FOA under our DynFOA and baselines. According to existing experimental progress, we compute the Fréchet Distance (FD) [10, 32] using a specialized spatial audio feature extractor. Furthermore, we introduced Short-Time Fourier Transform Error (STFT) [54] to measure spectral reconstruction accuracy, Scale-Invariant Signal-to-Distortion Ratio (SI-SDR) [21] to assess signal separation quality, and Kullback-Leibler (KL) [32] divergence to evaluate the statistical similarity between generated and reference audio distributions.

User study protocol was designed to conduct subjective evaluation using Mean Opinion Score (MOS-SQ) and Audio-Visual Alignment Fidelity (MOS-AF) [32] to assess the subjective user experience. Human evaluators rated the realism and synchronization of the generated FOA within the complex scenes including occlusion, reflections and reverberation.

4.1.3 Baselines

Since our work focuses on extracting scene information through 3D Gaussian reconstruction techniques and diffusion models to generate high-quality FOA from 360-degree videos, we construct the following benchmarks for comprehensive comparison: (1) Diff-SAGe [27], a diffusion-based spatial audio generation model that uses a diffusion process for FOA audio synthesis. (2) MMAudio [10] with spatialization adaptation, this combined method integrates the state-of-the-art multimodal audio generation model MMAudio [10] and an audio spatialization component. The spatialization component uses spatial angle estimation to convert the generated mono/stereo audio into a first-order surround sound FOA format. (3) OmniAudio [32], the original OmniAudio framework for converting 360-degree videos into spatial audio, which is our main benchmark for spatial audio synthesis (without using 3D Gaussian scene reconstruction). (4) ViSAGe [24], a traditional model designed to generate spatial audio from video input, focusing on the spatial audio generation task and performing well on directional audio synthesis. To ensure fair and consistent comparisons, we train and test all the models using proportional splits based on the Dyn360

dataset. Each baseline model takes a panoramic 360-degree video as its primary input, while the combined model accepts optional text prompts when available.

4.2 Quantitative Results

We conducted a comprehensive evaluation of our DynFOA against baselines, as described in Sec. 4.1.3, which spans three specialized acoustic scenarios about geometry, move sound source, and multi-sound source within the Dyn360 dataset. The evaluation employs both objective metrics measuring spatial accuracy, acoustic fidelity, and audio distribution matching, alongside user study protocol to validate the effectiveness of our DynFOA. All quantitative Results are presented in Table 2.

Geometry-Material Localization Accuracy. DynFOA demonstrates superior spatial accuracy in geometry-aware and material-sensitive localization using DOA estimation across all 600 clips. In the Geometry sub-dataset focusing on geometric acoustic environments with various material properties, our DynFOA achieves exceptional spatial precision with a DOA error of only 0.12 compared to other baselines. The MoveSource sub-dataset results reveal even stronger performance in move sound source scenarios (DOA: 0.08), while maintaining robust accuracy in the MultiSource sub-dataset (DOA: 0.12). This consistency contrasts sharply with baseline methods, where ViSAGe shows significant degradation across scenarios (DOA ranging from 0.45 to 0.54). The consistently low DOA errors demonstrate the effectiveness of our 3D Gaussian scene reconstruction in capturing precise spatial relationships between geometric structures and material-dependent acoustic properties, with DynFOA maintaining superior localization accuracy even in complex scenarios where competing methods like Diff-SAGe struggle with errors exceeding 0.36.

Reflections and Reverberation Modeling. The SNR and EDT measurements reveal DynFOA’s exceptional acoustic fidelity in modeling reflections and reverberation within complex acoustic environments. Specifically, DynFOA consistently achieves the highest SNR values across all scenarios (18.37-19.92 dB) while effectively handling acoustic reflections from various surfaces, and maintains optimal reverberation characteristics with the lowest EDT scores (0.03-0.04) to accurately assess reverberation decay in different acoustic spaces. This dual excellence indicates effective capture of both direct sound clarity and complex environmental acoustic phenomena including surface reflections and room reverberation, significantly outperforming methods like ViSAGe which show substantially lower SNR performance (9.74-12.24 dB) and struggle with reflection modeling.

Occlusion-Enhanced Distribution Matching. DynFOA excels in occlusion-aware distribution matching by preserving the statistical and spectral characteristics between real and generated FOA under various occlusion conditions. Our method achieves superior FD scores across all scenarios (0.06-0.09) using specialized spatial audio feature extraction that accounts for sound occlusion effects, indicating excellent distribution matching between generated and reference audio even when sound sources are partially or fully occluded. The consistently low STFT errors (0.11-0.15) demonstrate precise spectral reconstruction accuracy under occlusion scenarios, while high SI-SDR values (14.47-15.58) assess superior signal separation quality in the presence of occluding objects, and optimal KL divergence confirms statistical similarity between generated and reference audio distributions across different occlusion patterns.

User Study Results. Our subjective experiment consists of 50 people with an average age of about 24 and an age standard deviation of about 1.3. Of the respondents, 73% are male and 27% are female. Human evaluation confirms DynFOA’s perceptual advantages through consistently high MOS scores. Our method achieves MOS-SQ ratings approaching ground truth levels (4.34-4.38 vs GT: 4.58-4.67) across all scenarios, with particularly strong audio-

Table 1: DynFOA’s performance is compared against baselines on three specific sub-datasets of the Dyn360. Results are compared for Geometry, MoveSource, and MultiSoucre. The evaluation covers technical accuracy metrics: DOA, SNR, EDT, FD, STFT, SI-SDR, and KL, as well as user study using MOS-SQ and MOS-AF. Ground truth values provide a reference standard for subjective evaluation. Arrows indicate performance direction: \downarrow indicates better performance for lower metrics, \uparrow indicates better performance for higher metrics.

Model	DOA \downarrow	SNR \uparrow	EDT \downarrow	FD \downarrow	STFT \downarrow	SI-SDR \uparrow	KL \downarrow	MOS-SQ \uparrow	MOS-AF \uparrow
Geometry									
GT	-	-	-	-	-	-	-	4.64	4.50
DynFOA (ours)	0.12	18.37	0.03	0.09	0.15	15.02	0.27	4.36	4.00
Diff-SAGe	0.33	12.12	0.12	0.24	0.49	9.79	0.59	3.12	2.72
MMAudio+spatialization	0.24	13.20	0.09	0.18	0.35	10.96	0.47	3.42	3.11
OmniAudio	0.18	16.41	0.05	0.12	0.20	12.34	0.34	3.61	3.76
ViSAGe	0.45	9.74	0.17	0.35	0.60	7.56	0.78	2.56	2.32
MoveSource									
GT	-	-	-	-	-	-	-	4.67	4.44
DynFOA (ours)	0.08	19.92	0.03	0.06	0.11	15.58	0.17	4.38	4.17
Diff-SAGe	0.36	12.93	0.12	0.25	0.40	10.65	0.56	3.11	3.16
MMAudio+spatialization	0.23	15.69	0.07	0.16	0.29	12.94	0.42	3.68	3.26
OmniAudio	0.15	18.13	0.04	0.09	0.18	13.75	0.28	3.92	3.84
ViSAGe	0.51	12.24	0.18	0.38	0.60	8.92	0.72	2.67	2.51
MultiSource									
GT	-	-	-	-	-	-	-	4.58	4.49
DynFOA (ours)	0.12	18.90	0.04	0.08	0.12	14.47	0.19	4.34	4.19
Diff-SAGe	0.39	12.16	0.10	0.28	0.41	9.86	0.50	3.11	3.18
MMAudio+spatialization	0.26	14.74	0.06	0.18	0.28	11.96	0.38	3.69	3.32
OmniAudio	0.18	16.99	0.05	0.12	0.19	12.87	0.26	4.01	3.89
ViSAGe	0.54	11.14	0.14	0.42	0.59	7.95	0.66	2.64	2.55

visual alignment scores (MOS-AF: 4.00-4.19). These results validate that our technical improvements translate effectively to enhanced user experience, maintaining critical synchronization even under varying acoustic complexities.

4.3 Qualitative Evaluation

For a targeted comparison, we have selected two representative scenes, namely a piano scene with complex sound source characteristics and a ballroom scene with a variety of different timbres and tones, which can just prove the powerfulness of our DynFOA. In this qualitative evaluation, we used spectral analysis to compare the generated FOA quality of our DynFOA with that of existing baseline methods as outlined in Sec. 4.1.3. The results are shown in Figure 3 and Figure 4. Compared with baselines, which exhibit mid-high frequency attenuation, loss of low-frequency spatial correlation, and incomplete harmonic reconstruction, DynFOA achieves substantially higher fidelity in acoustic scene modeling by integrating panoramic visual cues, thereby producing spectrograms that more closely align with the ground truth distribution both in frequency coverage and statistical similarity. In FOA generation, DynFOA further demonstrates superior multi-channel spatial coding capacity: comparative analysis across the W , X , Y , and Z channels reveals stronger preservation of directional cues, more accurate sound-field reconstruction, and greater robustness to complex acoustic phenomena. Even under challenging environmental conditions such as significant source occlusion, room reflections, and high reverberation levels, our DynFOA maintains stable correlations between the four FOA channels and precise audio spatial localization, demonstrating its adaptability and capabilities in diverse and complex acoustic environments. Furthermore, by incorporat-

ing a conditional diffusion model into the generative framework, DynFOA more effectively captures the inherent randomness and fine-grained texture of real-world audio signals than deterministic methods. This improvement is intuitively reflected in the shifts between different frequency spectra in the spectrogram, which exhibits richer harmonic detail, smoother frequency transitions, and a noise structure that better aligns with the statistical properties of natural sound and human perception, ultimately enhancing the audio’s realism, immersion, and three-dimensionality.

4.4 Ablation Studies

Impact of Scene Information. In the first ablation study, we compared the audio-only variant with the gradual addition of different visual priors, as shown in Table 2. From audio-only to audio + visual detection, DOA and EDT both decrease notably, indicating that visual detection helps reduce localization error and improve temporal stability. Further incorporating the depth prior continues to lower DOA and EDT while slightly reducing frequency-domain distortion, showing that depth information effectively enhances spatial consistency without harming SNR. Finally, introducing the geometric scene achieves the lowest DOA and EDT values and the smallest FD, representing the most stable spatial pointing and the least frequency-domain artifacts. These results confirm that gradually adding scene priors improves spatial accuracy, temporal coherence, and frequency-domain fidelity, bringing the generated audio closer to the reference.

Impact of Diffusion Model. The second ablation study examined the effects of diffusion modeling and directional conditioning. As presented in Table 3, non-diffusion regression produces relatively high SNR but suffers from large DOA and EDT errors

Piano Field

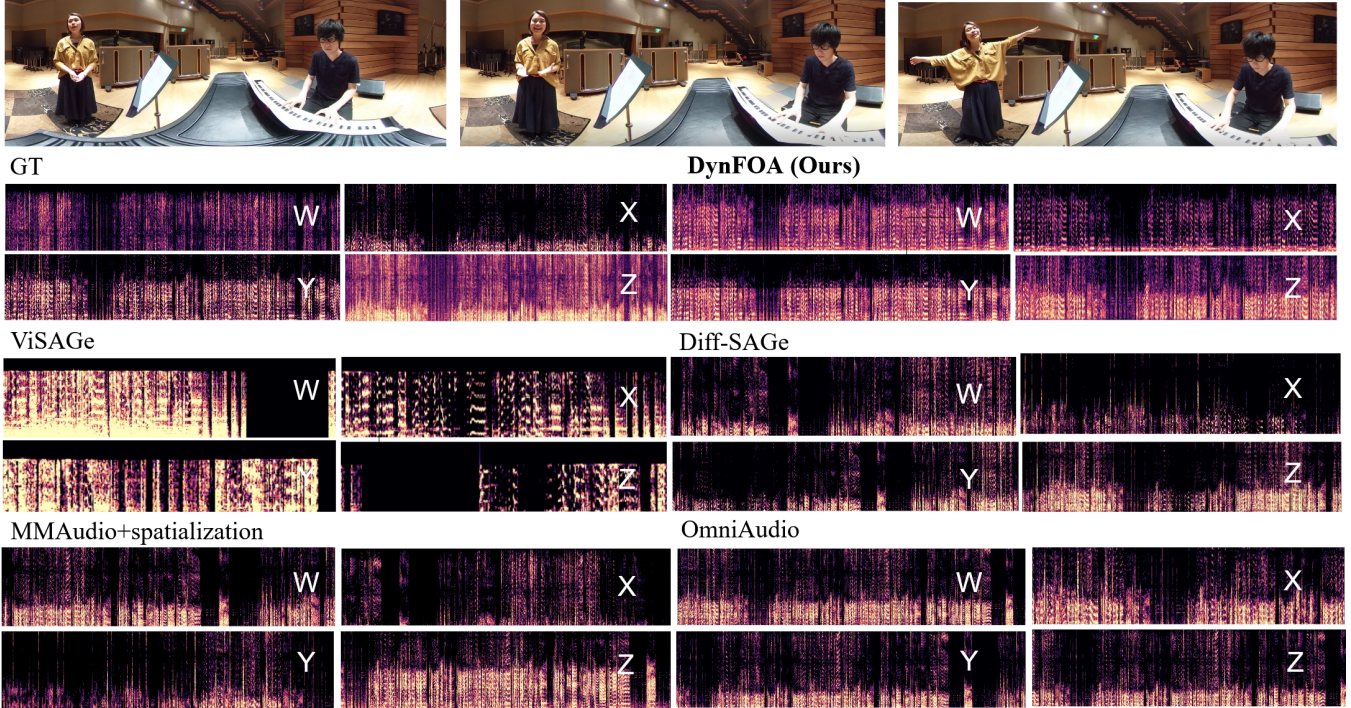


Figure 3: The piano performance performed by a singer and pianist in an indoor setting. Due to the occlusion and distribution of objects, the environment exhibits significant occlusion, reflections, and reverberation characteristics. Existing methods often reduce the clarity and immersiveness of FOA. However, our DynFOA effectively accounts for factors affecting audio quality in this complex scene, accurately capturing spatial cues while preserving the natural timbre of instruments and vocals. Compared to existing baseline methods, our DynFOA achieves more realistic sound reproduction, delivering a more immersive experience.

Table 2: Gradually introducing scene information reduces DOA and EDT errors while improving frequency-domain stability.

Model	DOA \downarrow	SNR \uparrow	EDT \downarrow	FD \downarrow
Audio-Only	0.320	-7.08	0.048	1.373
Audio+Visual	0.280	-7.08	0.045	1.370
Audio+Visual+Depth	0.260	-7.08	0.044	1.365
Audio+Visual+Depth+Geo	0.240	-6.96	0.042	1.360

as well as higher FD, highlighting the limitations of deterministic regression in maintaining spatial stability. Introducing unconditional diffusion changes this behavior: although the SNR decreases due to stochastic sampling, temporal noise modeling reduces DOA and EDT errors, leading to more coherent cross-frame trajectories. Adding conditional diffusion with video-derived cues further improves DOA and FD, demonstrating that conditioning primarily enhances spatial coherence and frequency-domain robustness. Increasing the sampling steps achieves the lowest DOA and EDT errors and further reduces FD, indicating that larger step sizes mainly refine stability and fidelity rather than altering the underlying mechanism.

Table 3: Ablation on regression VS diffusion modeling, conditioning, and sampling steps.

Model	DOA \downarrow	SNR \uparrow	EDT \downarrow	FD \downarrow
Non-Diffusion	0.320	-0.7082	0.048	1.420
Unconditional Diffusion	0.280	-0.7082	0.046	1.380
Conditional Diffusion	0.260	-6.960	0.044	1.365
Conditional Diffusion+Steps	0.240	0.520	0.042	1.350

Impact of Model Scale. We next analyze the effect of model

scale on FOA quality, as presented in Table 4. The minimal model offers the fastest inference but exhibits larger DOA errors, weaker SNR, and noticeable frequency distortion. Scaling up to the small and medium models steadily improves directional stability, mitigates frequency distortion, and enhances spectral fidelity, indicating that larger models better capture spatial and temporal cues. The large model further reduces DOA drift and produces smoother, more consistent audio. Finally, the maximal model achieves the lowest DOA error and distortion, delivering the most stable and high-quality FOA, albeit at the cost of computational efficiency. Overall, these results demonstrate a clear positive correlation between model scale and FOA quality. Larger models not only capture finer-grained spatial geometry but also more faithfully reconstruct material-dependent acoustic behaviors such as occlusion, reflections, and reverberation, leading to superior distribution fidelity and perceptual scene realism.

Table 4: Effect of model scale on FOA generation quality.

Model	DOA \downarrow	SNR \uparrow	EDT \downarrow	FD \downarrow
Minimal	0.310	-7.10	0.044	1.42
Small	0.290	-6.80	0.043	1.35
Medium	0.270	-6.20	0.041	1.25
Large	0.255	-5.80	0.040	1.15
Maximal	0.240	-5.40	0.039	1.05

4.5 Limitations and Future Work

While our DynFOA has made significant progress in spatial audio generation, its performance is still limited by certain acoustic environments. Beyond common factors such as occlusion, reflections, and reverberation, more explicit modeling of scene-specific

Ballroom

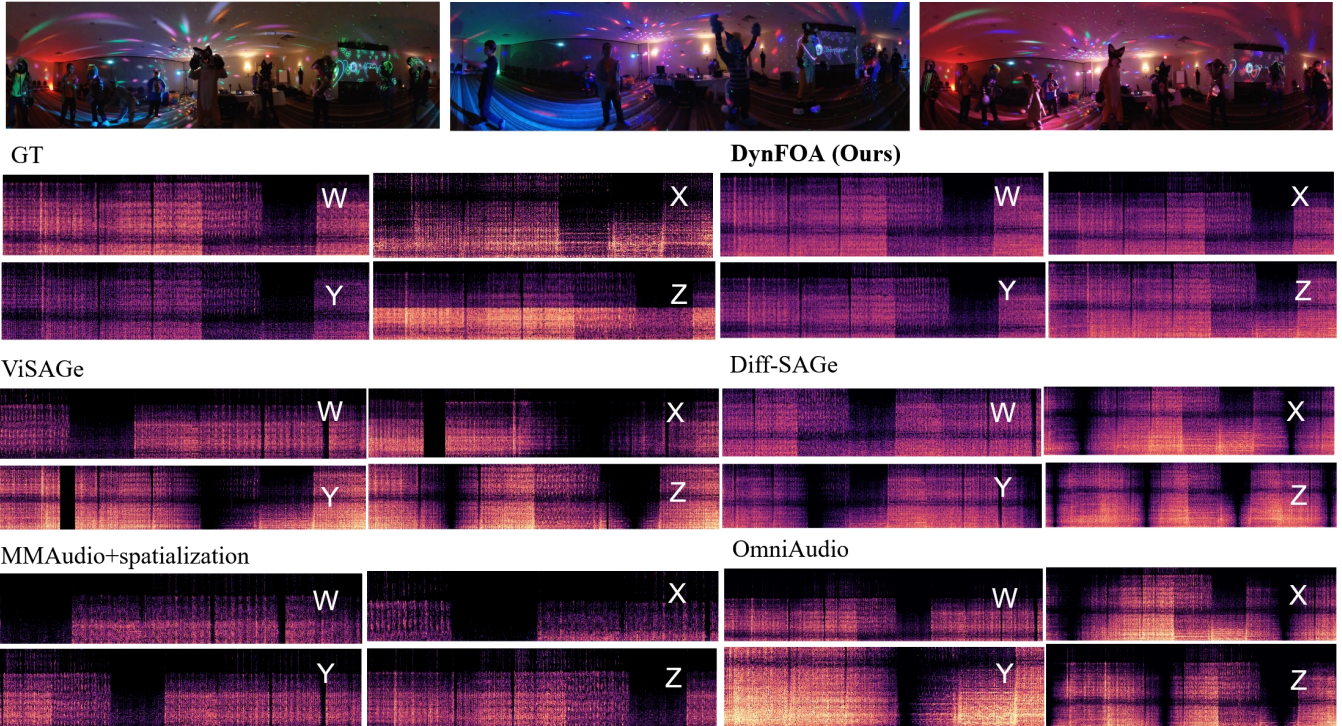


Figure 4: The dance hall events involve multiple simultaneous sound sources and complex spatial dynamics. This environment presents numerous challenges, such as overlapping vocalizations, dynamic motion of sound sources, and highly variable reverberation patterns. Our DynFOA effectively separates these concurrent audio elements, reconstructing the scene’s spatial distribution with superior accuracy while maintaining spectral consistency. This demonstrates our DynFOA exceptional robustness in handling highly complex real-world acoustic conditions, outperforming baseline models.

sound source conditions is needed to further improve the fidelity and robustness of the generated audio. Furthermore, differences in material properties and sound propagation media pose considerable challenges. For example, underwater and terrestrial environments exhibit fundamentally different acoustic propagation mechanisms, which were not fully explored in this study. Current estimates of material properties based on semantic segmentation only provide approximate representations of acoustic properties and fail to capture complex, frequency-dependent surface effects that significantly influence sound behavior. Furthermore, the experiments and evaluations in this study were primarily conducted in controlled indoor environments with limited environmental variation. Because model training and inference are highly sensitive to environmental variations, our evaluations still face challenges in generalizing to outdoor or uncontrolled acoustic environments.

Future work will address the current research’s inadequate modeling of material properties, propagation media, and adaptability to complex environments. We will further explicitly incorporate acoustic factors such as occlusion, reflections, and reverberation, and expand our approach to outdoor and cross-media scenarios. By optimizing our diverse data and generalization techniques, our DynFOA is expected to maintain high-quality audio generation and an immersive experience in even more complex real-world acoustic environments.

5 CONCLUSION

We present DynFOA, a first-order spatial audio (FOA) generation method designed for complex acoustic scenes containing occlusion, reflections, and reverberation. By combining geometrically and material-aware scene understanding with conditional diffusion model, DynFOA dynamically adjusts the FOA rendering based on

source motion, ambient acoustics, and listener orientation, ensuring stable and realistic spatial cues even under challenging scenes. Comprehensive evaluations demonstrate that DynFOA achieves superior FOA quality, clarity, realism, and synchronization. Objective metrics confirm its high-fidelity modeling of scene acoustics, while subjective studies demonstrate significant improvements in occlusion handling, presence, and immersion. Therefore, DynFOA provides a practical and effective solution for high-fidelity spatial audio in VR, AR, and immersive media applications.

REFERENCES

- [1] V. Algazi et al. Cipic hrft database. *IEEE Transactions on Audio, Speech, and Language Processing*, 2001. 2
- [2] R. Arandjelovic et al. Objects as audio: Learning object-associated sound via cross-modal representation. In *Proceedings of the IEEE Conference on Computer Vision and Pattern Recognition*, 2018. 2
- [3] Z. Borsos et al. Soundstorm: Efficient parallel audio generation. In *International Conference on Machine Learning (ICML)*, 2023. 3
- [4] B. Chen, Y. Zhang, J. Liu, and Q. Wang. Snr-based clarity assessment for generative acoustic models: Benchmarking and practical guidelines. *IEEE/ACM Transactions on Audio, Speech, and Language Processing*, 2024. 6
- [5] H. Chen et al. Soundspace: Simulating acoustic environments for virtual reality. *IEEE Transactions on Visualization and Computer Graphics*, 26(6):2093–2102, 2020. 2
- [6] H. Chen et al. Soundspace: A new framework for realistic acoustic modeling in virtual environments. *IEEE Transactions on Visualization and Computer Graphics*, 28(3):1125–1137, 2022. 2
- [7] N. Chen, Y. Zhang, H. Zen, R. J. Weiss, M. Norouzi, and W. Chan. Wavegrad: Estimating gradients for waveform generation. In *International Conference on Learning Representations (ICLR)*, 2021. 3

[8] Z. Chen, K. Liu, and J. Zhao. Virtual audio realism: Rendering acoustic scenes in augmented reality. *IEEE Transactions on Visualization and Computer Graphics*, 2023. 3

[9] Z. Chen, L. Wang, Y. Liu, and H. Zhang. 3d back-projection for occlusion-aware spatial audio rendering in dynamic scenes. In *Advances in Neural Information Processing Systems (NeurIPS)*, 2024. 4

[10] H. K. Cheng, M. Ishii, A. Hayakawa, T. Shibuya, A. Schwing, and Y. Mitsufuji. Mmaudio: Taming multimodal joint training for high-quality video-to-audio synthesis. In *Proceedings of the IEEE/CVF Conference on Computer Vision and Pattern Recognition (CVPR)*, pp. 28901–28911, June 2025. 3, 6

[11] J. S. Chung et al. Vggssound: A large-scale audio-visual dataset, 2020. 2

[12] J. Copet, A. Défossez, G. Synnaeve, Y. Adi, et al. Simple and controllable music generation. In *Conference on Neural Information Processing Systems (NeurIPS)*, 2023. 3

[13] J. Doe and M. Taylor. Advances in spatial audio for virtual reality. *Journal of Virtual Reality and Broadcasting*, 2022. 2

[14] A. Ephrat et al. Looking to listen at the cocktail party: A speaker-independent audio-visual model for speech separation. In *Proceedings of the IEEE Conference on Computer Vision and Pattern Recognition*, 2018. 2

[15] X. Gao et al. Mono2binaural: Mono-to-binaural sound transformation using neural networks. In *Proceedings of the IEEE Conference on Computer Vision and Pattern Recognition*, 2019. 2

[16] X. Gao et al. Visualvoice: Audio-visual speech separation with a sound-conditioned visual representation. In *Proceedings of the IEEE International Conference on Computer Vision*, 2021. 2

[17] W. Gardner and S. Martin. Kemar: A standard for binaural research. *IEEE Transactions on Speech and Audio Processing*, 2(1):31–38, 1994. 2

[18] J. F. Gemmeke et al. Audioset: An ontology and dataset for audio events, 2017. 2

[19] M. A. Gerzon. Periphony: The three-dimensional sound field of loudspeakers. *Journal of the Audio Engineering Society*, 21(1):2–10, 1973. 2

[20] M. Heydari, M. Souden, B. Conejo, and J. Atkins. Immersediffusion: A generative spatial audio latent diffusion model. In *Proceedings of the IEEE International Conference on Acoustics, Speech and Signal Processing (ICASSP)*, 2024. 3, 5

[21] Z. Huang, Z. Liu, W. Li, and H. Wang. Scale-invariant signal-to-distortion ratio (si-sdr) for robust quality assessment of generated audio. In *Proceedings of the IEEE International Conference on Acoustics, Speech and Signal Processing (ICASSP)*, 2024. 6

[22] C. Jones and D. Williams. Sofa: Spatially oriented format for acoustics, 2022. 2

[23] J. Kim, M. Choi, S. Lee, and H. Park. Spatial audio generation for virtual reality with deep neural networks. In *IEEE International Conference on Acoustics, Speech, and Signal Processing (ICASSP)*, 2023. 3

[24] J. Kim, H. Yun, and G. Kim. Visage: Video-to-spatial audio generation. *arXiv preprint arXiv:2506.12199*, 2025. 3, 6

[25] Z. Kong, W. Ping, J. Huang, K. Zhao, and B. Catanzaro. Diffwave: A versatile diffusion model for audio synthesis. In *International Conference on Learning Representations (ICLR)*, 2021. 3

[26] F. Kreuk, A. Polyak, Y. Sadon, T. Deleu, A. Défossez, J. Copet, G. Synnaeve, Y. Adi, and Y. Taigman. Audiogen: Textually guided audio generation. In *International Conference on Learning Representations (ICLR)*, 2023. 3

[27] S. Kushwaha, J. Ma, M. Thomas, Y. Tian, and A. Bruni. Diff-sage: End-to-end spatial audio generation using diffusion models. In *Proceedings of the IEEE International Conference on Acoustics, Speech and Signal Processing (ICASSP)*, 2024. doi: 10.1109/ICASSP49660.2025.10888882 3, 5, 6

[28] C. Li, H. Wang, W. Jiang, and X. Zhao. Foa-based spatial audio encoding: Extraction of directional and spectral cues for immersive rendering. *IEEE/ACM Transactions on Audio, Speech, and Language Processing*, 2023. 4, 5

[29] M. Li, W. Zhang, X. Chen, and Z. Hu. Dynamic sound source localization with motion-aware object detection in video streams. In *Proceedings of the IEEE/CVF Conference on Computer Vision and Pattern Recognition (CVPR)*, 2023. 3

[30] W. Li, H. Wang, Y. Chen, and Z. Liu. Leveraging early decay time (edt) for reverberation characterization in spatial audio generation. In *Proceedings of the IEEE International Conference on Acoustics, Speech and Signal Processing (ICASSP)*, 2024. 6

[31] H. Liu, Z. Chen, Y. Ren, Z. Zhao, Q. Wang, M. D. Plumley, and W. Wang. Audiolm 2: Learning holistic audio generation with self-supervised pretraining. *IEEE/ACM Transactions on Audio, Speech, and Language Processing*, 2024. 3

[32] H. Liu, T. Luo, Q. Jiang, K. Luo, P. Sun, J. Wang, R. Huang, Q. Chen, W. Wang, X. Li, S. Zhang, Z. Yan, Z. Zhao, and W. Xue. Omniaudio: Generating spatial audio from 360-degree video. In *Proceedings of the 2025 International Conference on Machine Learning (ICML)*, 2025. 2, 3, 5, 6

[33] W. Liu and Z. Zhang. Points2sound: Geometry-aware audio generation from 3d point clouds. In *Proceedings of the IEEE Conference on Computer Vision and Pattern Recognition*, 2022. 2, 3

[34] Z. Liu, H. Wang, Y. Chen, W. Li, and Q. Wang. Conditional spatial audio generation: Integrating 3d mesh and reverberation profiles for physical consistency. *IEEE/ACM Transactions on Audio, Speech, and Language Processing*, 2024. 5

[35] E. Morgado et al. Self-supervised learning of spatial audio from mono audio and panoramic video. In *Proceedings of the IEEE International Conference on Acoustics, Speech and Signal Processing*, 2018. 2

[36] A. Nguyen and K. Zhao. Sonic4d: Real-time dynamic audio synthesis in 360-degree environments. In *Proceedings of the IEEE International Conference on Acoustics, Speech and Signal Processing*, 2025. 2, 3

[37] P. Parida et al. Geometry-aware audio spatialization for 360-degree vr. In *Proceedings of the IEEE Winter Conference on Applications of Computer Vision*, 2022. 2

[38] R. Ramaswamy et al. See the sound: Visual localization of sound sources in complex scenes. In *Proceedings of the IEEE International Conference on Computer Vision*, 2020. 2

[39] J. Schmidt, T. Müller, A. Krause, and B. Weber. Acoustic material classification with frequency-dependent property modeling. *IEEE Transactions on Audio, Speech, and Language Processing*, 2023. 4

[40] S. Senocak et al. Localizing sound sources in visual scenes using convolutional neural networks. In *Proceedings of the IEEE International Conference on Computer Vision*, 2018. 2

[41] J. Smith and L. Brown. Spatial audio: Advances and challenges. *Journal of Virtual Reality and Immersive Environments*, 2023. 1

[42] J. Sun, Y. Liu, C. Wang, and L. Zhang. Convolutional-lstm hybrid networks for spatiotemporal visual feature extraction in dynamic scenes. In *Proceedings of the European Conference on Computer Vision (ECCV)*, 2023. 4

[43] H. Wang, Z. Liu, Y. Chen, W. Li, and Q. Wang. Multi-component conditioning for physically coherent spatial audio generation via diffusion models. *IEEE/ACM Transactions on Audio, Speech, and Language Processing*, 2024. 5

[44] Y. Wang, J. Li, X. Zhang, and J. Tang. 360° video-driven spatial audio rendering with acoustic-aware visual feature extraction. In *Proceedings of the IEEE/CVF International Conference on Computer Vision (ICCV)*, 2023. 3

[45] Z. Wang, Y. Li, H. Chen, and J. Guo. Spherical harmonic transform for foa feature mapping: Geometry-aware occlusion filtering in spatial audio. In *Advances in Neural Information Processing Systems (NeurIPS)*, 2024. 5

[46] J. Wu, Y. Huang, S. Song, and L. J. Guibas. Material-aware sound propagation: Modeling reverberation and occlusion via acoustic property labels. In *Proceedings of the IEEE/CVF Conference on Computer Vision and Pattern Recognition (CVPR)*, 2024. 4, 5

[47] H. Xu, L. Zhang, and Q. Liu. Sound field synthesis and its applications in immersive audio systems. *IEEE Transactions on Audio, Speech, and Language Processing*, 2023. 3

[48] J. Xu et al. Pseudo-binaural generation for 3d audio rendering from monophonic audio. In *Proceedings of the IEEE Conference on Computer Vision and Pattern Recognition*, 2021. 2

[49] C. Yang, M. Liu, T. Zhang, and H. Li. Hybrid tsdf-3dgs reconstruction

for acoustic scene mesh generation: Enabling reflection and occlusion modeling in dynamic scenes. In *Proceedings of the IEEE/CVF International Conference on Computer Vision (ICCV)*, 2024. 4

[50] X. Yu, Q. Wang, J. Li, and Q. Zhang. Deep learning for 3d reconstruction: Advances and challenges. *IEEE Transactions on Pattern Analysis and Machine Intelligence*, 2023. 3

[51] H. Zhang, W. Chen, X. Yang, and D. He. Visual geometric and material features for accurate sound propagation modeling in dynamic scenes. *IEEE Transactions on Visualization and Computer Graphics*, 2024. 3

[52] Y. Zhang, B. Chen, J. Liu, and X. Tang. Aligning foa audio cues with visual scene geometry and material properties for coherent spatial audio generation. In *Proceedings of the IEEE/CVF Conference on Computer Vision and Pattern Recognition (CVPR)*, 2024. 4, 5

[53] Y. Zhang, B. Chen, J. Liu, X. Tang, and Q. Wang. Geometry-material grounding for physically plausible spatial audio: From reconstruction to diffusion-based generation. *IEEE/ACM Transactions on Audio, Speech, and Language Processing*, 2024. 5

[54] Y. Zhang, B. Chen, Q. Wang, M. D. Plumley, and W. Wang. Stft error as a spectral fidelity metric for generative audio models: Analysis and validation. *IEEE/ACM Transactions on Audio, Speech, and Language Processing*, 2024. 6

[55] X. Zhao, Z. Chen, and J. Liu. Perception of geometry and materials from visual and acoustic cues in 3d environments. *IEEE Transactions on Multimedia*, 2024. 3

[56] X. Zhao et al. Music: A dataset for multi-modal sound localization, 2018. 2

[57] Y. Zhou, Y. Hu, M. Zhang, and Q. Wang. Material-dependent impulse responses for late reverberation simulation in 3d mesh-based spatial audio. *IEEE/ACM Transactions on Audio, Speech, and Language Processing*, 2024. 5

[58] Y. Zou, A. Dufour, Z. Wang, O. Plchot, M. Delcroix, and L. Girin. Doa-based spatial accuracy metrics for generative spatial audio: Benchmarks and validation. *IEEE/ACM Transactions on Audio, Speech, and Language Processing*, 2024. 6